Cell

Androgen Receptor Regulates a Distinct Transcription Program in Androgen-Independent Prostate Cancer

Qianben Wang,[1,2,14,*] Wei Li,[3,14] Yong Zhang,[4] Xin Yuan,[5] Kexin Xu,[1] Jindan Yu,[6] Zhong Chen,[2] Rameen Beroukhim,[1,7] Hongyun Wang,[5] Mathieu Lupien,[1,13] Tao Wu,[8] Meredith M. Regan,[4] Clifford A. Meyer,[4] Jason S. Carroll,[9] Arjun Kumar Manrai,[4] Olli A. Jänne,[10] Steven P. Balk,[5] Rohit Mehra,[6] Bo Han,[6] Arul M. Chinnaiyan,[6] Mark A. Rubin,[11] Lawrence True,[12] Michelangelo Fiorentino,[1] Christopher Fiore,[1] Massimo Loda,[1] Philip W. Kantoff,[1] X. Shirley Liu,[4,*] and Myles Brown[1,*]

[1]Department of Medical Oncology, Dana-Farber Cancer Institute and Harvard Medical School, Boston, MA 02115, USA
[2]Department of Molecular and Cellular Biochemistry and the Comprehensive Cancer Center, Ohio State University College of Medicine, Columbus, OH 43210, USA
[3]Division of Biostatistics, Dan L. Duncan Cancer Center and Department of Molecular and Cellular Biology, Baylor College of Medicine, Houston, TX 77030, USA
[4]Department of Biostatistics and Computational Biology, Dana-Farber Cancer Institute and Harvard School of Public Health, Boston, MA 02115, USA
[5]Cancer Biology Program, Hematology-Oncology Division, Department of Medicine, Beth Israel Deaconess Medical Center and Harvard Medical School, Boston, MA 02215, USA
[6]Department of Pathology, University of Michigan Medical School, Ann Arbor, MI 48109, USA
[7]Broad Institute of Harvard and MIT, Cambridge, MA 02139, USA
[8]Department of System Biology, Harvard Medical School, Boston, MA 02115, USA
[9]Cancer Research UK, Cambridge Research Institute, Robinson Way, Cambridge CB2 0RE, UK
[10]Biomedicum Helsinki, Institute of Biomedicine (Physiology), University of Helsinki, Helsinki, FI-00014, Finland
[11]Department of Pathology and Laboratory Medicine, Weill Cornell Medical College, New York, NY 10021, USA
[12]Department of Pathology, University of Washington Medical Center, Seattle, WA 98195, USA
[13]Present address: Department of Genetics, Norris Cotton Cancer Center, Dartmouth Medical School, Lebanon, NH 03756, USA
[14]These authors contributed equally to this work
*Correspondence: qianben.wang@osumc.edu (Q.W.), xsliu@jimmy.harvard.edu (X.S.L.), myles_brown@dfci.harvard.edu (M.B.)
DOI 10.1016/j.cell.2009.04.056

SUMMARY

The evolution of prostate cancer from an androgen-dependent state to one that is androgen-independent marks its lethal progression. The androgen receptor (AR) is essential in both, though its function in androgen-independent cancers is poorly understood. We have defined the direct AR-dependent target genes in both androgen-dependent and -independent cancer cells by generating AR-dependent gene expression profiles and AR cistromes. In contrast to what is found in androgen-dependent cells, AR selectively upregulates M-phase cell-cycle genes in androgen-independent cells, including *UBE2C*, a gene that inactivates the M-phase checkpoint. We find that epigenetic marks at the UBE2C enhancer, notably histone H3K4 methylation and FoxA1 transcription factor binding, are present in androgen-independent cells and direct AR-enhancer binding and UBE2C activation. Thus, the role of AR in androgen-independent cancer cells is not to direct the androgen-dependent gene expression program without androgen, but rather to execute a distinct program resulting in androgen-independent growth.

INTRODUCTION

Androgens, functioning through the androgen receptor (AR), are essential for the initiation and progression of prostate cancer (Heinlein and Chang, 2004). Thus, androgen-ablation therapies, which involve surgical castration or the use of luteinizing hormone-releasing hormone (LHRH) agonists (or antagonists), have been the mainstay of treatment for advanced androgen-dependent prostate cancer (ADPC) for over 40 years. While such therapies initially lead to disease regression, in general, advanced prostate cancer ultimately progresses to an androgen-independent (AIPC) late stage that is refractory to current therapies (also termed ''castration-resistant prostate cancer'') (Debes and Tindall, 2004; Feldman and Feldman, 2001). As AR is expressed in the vast majority of both ADPC and AIPC (Heinlein and Chang, 2004; Scher and Sawyers, 2005) and decreasing levels of AR protein expression reduces both ADPC and AIPC growth in model systems (Chen et al., 2004; Haag et al., 2005; Heinlein and Chang, 2004), it appears AR signaling pathways play a critical role in both ADPC and AIPC.

AR is a member of nuclear hormone receptor superfamily that regulates target gene expression in a ligand-inducible manner (Mangelsdorf et al., 1995). Two well-characterized AR target genes in ADPC are prostate specific antigen (*PSA*) and the *TMPRSS2-ETS* fusion genes. Recent studies have demonstrated

that control of these target genes involves long-range, combinatorial regulation by AR, DNA-binding collaborating transcription factors and non-DNA binding co-regulatory factors (Shang et al., 2002; Wang et al., 2005; Wang et al., 2007). While the role of AR target genes in regulating cell-cycle progression in ADPC have yet to be fully defined, it is well understood that decreased ADPC growth after AR silencing and/or androgen deprivation primarily involves a block of the G1/S cell-cycle transition through AR-dependent regulation of cyclin D1, p21 and p27 (Comstock and Knudsen, 2007). In contrast, how AR regulates cell growth in AIPC is not known. Addressing this question is of clinical importance as it may lead to the identification of specific therapeutic targets for this lethal stage of the disease. By comparing the program of gene expression directly regulated by AR in a model of the progression of ADPC to AIPC and gene and protein expression from actual AIPC cases we find that AR selectively and directly upregulates a set of M-phase cell-cycle genes to promote AIPC growth.

RESULTS

M-phase Cell-Cycle Genes Are Upregulated Genes Both in a Cell Culture Model of AIPC and in Clinical AIPC Samples

To mimic the properties of clinical prostate cancer progression, we utilized LNCaP-abl (abl), an androgen-independent derivative of the androgen-dependent LNCaP prostate cancer cell line that was generated after long-term androgen deprivation (Culig et al., 1999). Consistent with its AIPC phenotype abl cells grow substantially more rapidly than LNCaP cells in hormone-depleted medium (see Figure S1A available with this article online). While the physiological androgen 5α-dihydrotestosterone (DHT) significantly increases LNCaP cell proliferation, it has little effect on abl cell growth (Figure S1A). To identify genes that might account for the androgen-independent growth of abl compared with LNCaP, we examined gene expression profiles of abl cells in the absence of DHT and LNCaP cells in the absence and presence of DHT treatment for 4 hr (Figure S1B) using Affymetrix U133 plus 2.0 expression arrays. Gene Ontology (GO) analysis of upregulated transcripts in abl compared with LNCaP in the absence of DHT showed that the top two enriched GO biological processes are "cell cycle" ($p = 2.8 \times 10^{-19}$, modified Fisher exact p value, hereinafter) and "mitotic cell cycle" ($p = 2.2 \times 10^{-17}$), suggesting that higher expression of cell-cycle genes, particularly M-phase genes, may contribute to AIPC growth. Interestingly, GO analysis of upregulated transcripts in abl compared with LNCaP cells treated with DHT for 4 hr also revealed that "M phase" ($p = 8.8 \times 10^{-22}$) and "Cell cycle" ($p = 1.4 \times 10^{-21}$) as top two enriched GO biological processes, suggesting that androgen does not directly increase cell-cycle gene transcription in LNCaP cells to promote their growth. This result is consistent with a recent study demonstrating that androgen induces LNCaP growth through mTOR activation and a post-transcriptional increase in Cyclin D protein level (Xu et al., 2006). We next investigated whether cell-cycles genes are also enriched in upregulated genes from clinical cases of AIPC compared with ADPC cases. This was accomplished by re-analyzing gene expression profiles of AIPC and ADPC from two clinical studies (Figure S1B) (Stanbrough et al., 2006; Varambally et al., 2005). In agreement with the cell line results, the most significantly enriched GO biological processes categories in clinical AIPC upregulated transcripts are also "cell cycle" (Varambally dataset, $p = 4.7 \times 10^{-15}$, and Stanbrough dataset, $p = 2.7 \times 10^{-23}$) and "mitotic cell cycle" (Varambally dataset, $p = 6.3 \times 10^{-16}$, and Stanbrough dataset, $p = 1.9 \times 10^{-22}$). These data demonstrate that expression of cell-cycle regulatory genes, primarily M-phase genes are enriched in AIPC and may promote AIPC growth.

AR Upregulates M-Phase Cell-Cycle Genes to Promote AIPC Growth

Given our finding that expression of specific cell-cycle genes are upregulated in abl compared with LNCaP and the requirement of AR for growth of both cell lines (Figure 1A), we hypothesized that AR promotes AIPC proliferation by upregulating specific cell-cycle genes. We next performed gene expression profiling to define AR-dependent genes in abl by transfection of a short interfering RNA (siRNA) against AR (siAR) or a control siRNA (siControl). As referents, we also performed gene expression analysis in LNCaP cells following AR silencing and in both cell lines over a time course of DHT stimulation (0, 4 hr, and 16 hr) (Figure 1B) (Wang et al., 2007). Unsupervised hierarchical clustering of the expression data clearly distinguished androgen-regulated genes and AR-regulated genes that reflect ligand-activated and basal AR activity, respectively (Figure 1B). Therefore, AR-regulated genes in AIPC are not the same as those regulated by androgen in ADPC (Figures 1C and S2). As AR silencing decreases abl cell proliferation (Figure 1A), we next focused on the AR upregulated genes in abl cells (i.e., siControl/siAR upregulated genes). Interestingly, GO analysis of 345 abl-specific AR upregulated transcripts ($q < 0.05$) (Figure 1C) revealed that "cell cycle" (52 transcripts, $p = 1.4 \times 10^{-9}$) and "mitotic cell cycle" (24 transcripts, $p = 8.0 \times 10^{-9}$) are the top two over-represented GO biological processes. Moreover, comparing these AR upregulated cell-cycle transcripts in abl cells with upregulated transcripts in clinical AIPC showed very significant overlaps (hypergeometric distribution, for cell-cycle transcripts: 36% ($p = 8.85 \times 10^{-3}$) overlap with Varambally dataset and 50.9% ($p = 1.05 \times 10^{-3}$) overlap with Stanbrough dataset; for M phase transcripts: 62.5% ($p = 1.20 \times 10^{-5}$) overlap with Varambally dataset and 91.7% ($p = 4.02 \times 10^{-10}$) overlap with Stanbrough dataset) (Figure 1D). In contrast to enriched "cell cycle" and "mitotic cell cycle" GO biological processes for abl-specific AR upregulated transcripts, the most significantly enriched GO biological processes for 23 LNCaP-specific basal AR upregulated transcripts and 435 LNCaP-specific transcripts upregulated by 4 hr DHT treatment (Figure 1C) are "cellular lipid metabolism" ($p = 7.7 \times 10^{-2}$) and "positive regulation of cellular process ($p = 9.7 \times 10^{-5}$)," respectively. In addition, 291 of 345 transcripts abl-specific AR upregulated transcripts ($q < 0.05$) have a higher AR induced gene expression fold change in abl than in LNCaP cells. GO analysis of these 291 genes also revealed that "cell cycle" ($p = 2.6 \times 10^{-9}$) and "mitotic cell cycle" ($p = 5.2 \times 10^{-9}$) as the top two enriched GO biological processes. Taken together these data suggest that AR selectively upregulates M-phase cell-cycle genes to promote AIPC growth.

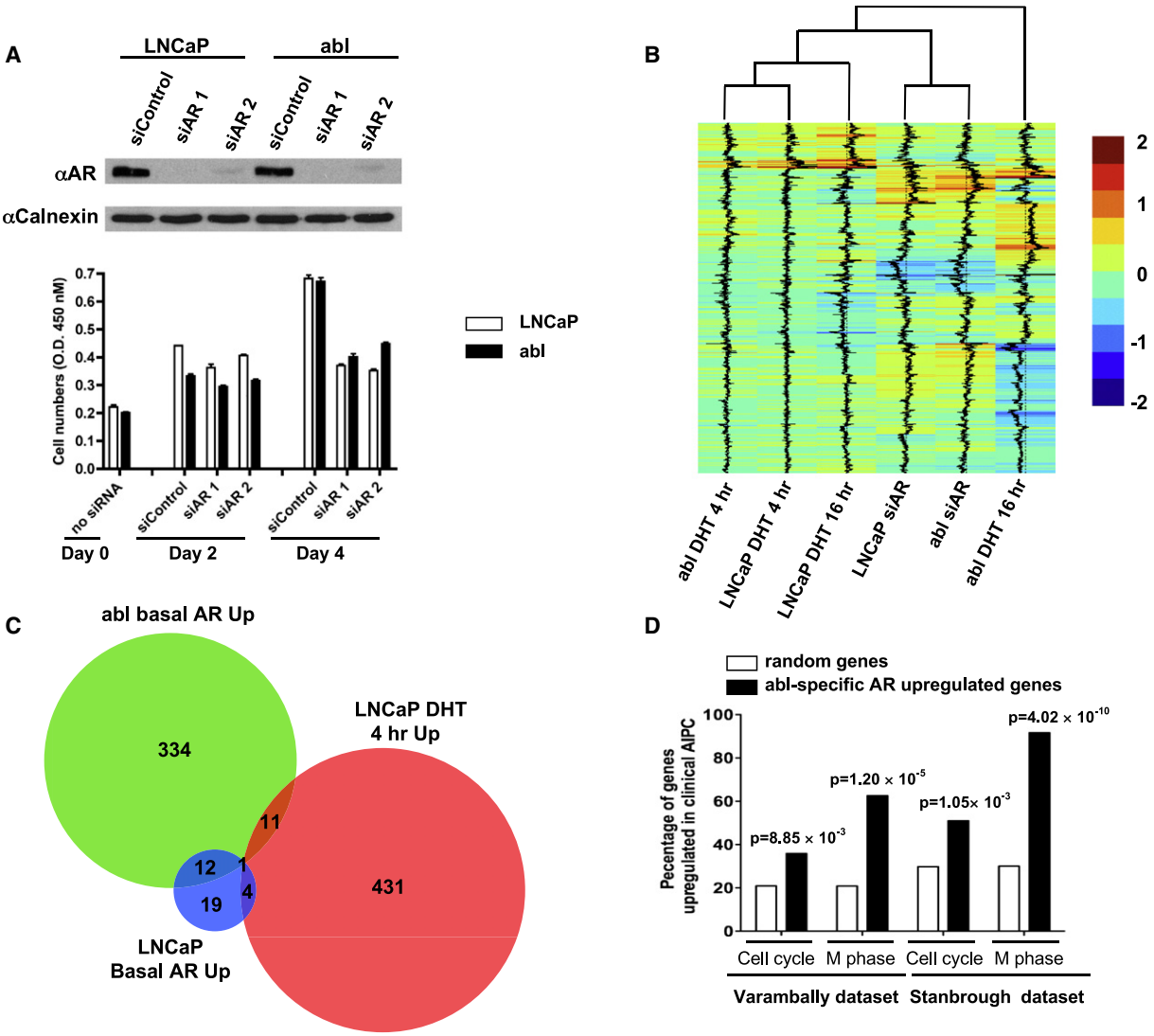

Figure 1. AR Silencing in abl Cells Significantly Decreases M-Phase Cell-Cycle Gene Expression

(A) AR silencing decreases both LNCaP and abl cell proliferation. LNCaP cells were cultured regular RPMI 1640 supplemented with 10% fetal bovine serum (FBS). abl cells were grown in phenol-red free RPMI 1640 supplemented with 10% charcoal/dextran-stripped FBS. Both cell lines were grown in the absence of supplemental DHT. Cells were transfected with two independent AR siRNA. The cell proliferation was measured on day 2 and day 4, after siRNA transfection, using the WST-1 assay (mean (n = 3) ± SE).

(B) Cluster analysis of genes differentially expressed ($q < 0.05$) by either DHT treatment and/or siAR transfection. Unsupervised hierarchical clustering of genes (rows) from cells in different conditions (columns) was performed. Brown and blue color represents upregulation and downregulation, respectively.

(C) A Venn diagram showing the basal AR upregulated genes in LNCaP and abl cells and DHT 4 hr upregulated genes in LNCaP cells.

(D) Comparison of abl-specific AR upregulated genes with upregulated genes in two clinical AIPC datasets (Stanbrough et al., 2006; Varambally et al., 2005).

Preferential AR Binding to the M-Phase Genes Leads to Higher Expression in AIPC

To investigate the underlying regulatory mechanism for the differential pattern of AR-regulated genes in AIPC and ADPC, we defined the AR cistrome by combining chromatin immunoprecipitation (ChIP) with tiled oligonucleotide microarrays across the entire human genome (ChIP-on-chip) in abl and LNCaP cells. Briefly, AR ChIP was first performed in abl and LNCaP cells. The ChIP-enriched DNA was then amplified and hybridized to Afftymetrix whole human genome tiling array sets. In order to increase the sensitivity of our approach (Johnson et al., 2008), we performed the AR ChIP-on-chip in the presence of DHT in both cell lines. Our strategy is to identify AR binding sites by ChIP-on-chip in the presence of androgen followed by the validation of sites of interest by directed ChIP in both the presence and absence of androgen. Using the MAT algorithm (Johnson et al., 2006), we identified 8,708 AR binding sites in LNCaP cells and 6,353 AR binding regions in abl cells based on a stringent false discovery rate (FDR) of 5% (Figure S3). As positive controls, we found that these included previously reported AR binding regions

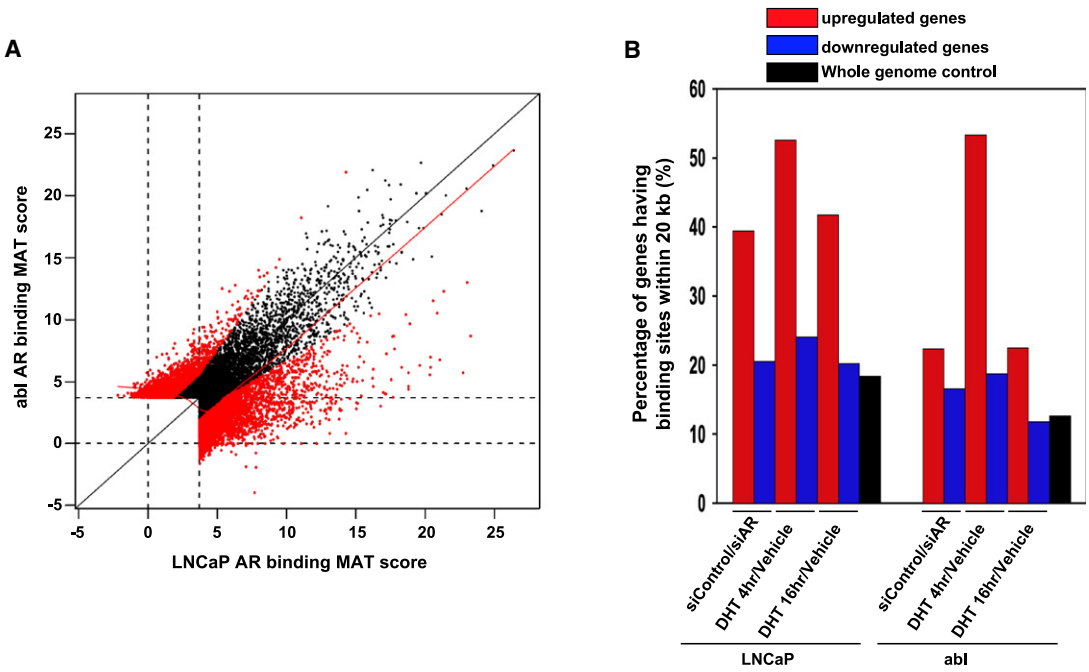

Figure 2. AR Directly Regulates Basal and Activated AR Upregulated Genes in LNCaP and abl Cells

(A) Comparison of AR whole genome binding in LNCaP and abl cells. Triplicate AR whole genome ChIP-on-chip was performed in LNCaP and abl cells treated with DHT for 4 hr. MAT was used to detect AR ChIP-enriched regions. Each dot represents a binding site. Red dots represents differential binding while dark dots refers to nondifferential binding.

(B) Correlation of AR binding to differential gene expression in LNCaP and abl cells. The graph represents the percentage of genes having AR binding sites with 20 kb of the transcription start sites. The enrichment of AR binding near the TSS of upregulated genes over whole genome background is statistically significant in both LNCaP and abl cells (Chi-square test, LNCaP (siControl/siAR, $p = 1.82 \times 10^{-3}$; DHT 4 hr/vehicle, $p = 2.58 \times 10^{-71}$; DHT 16 hr/vehicle, $p = 9.57 \times 10^{-65}$), abl (siControl/siAR, $p = 6.90 \times 10^{-8}$; DHT 4 hr/vehicle, $p = 7.91 \times 10^{-46}$; DHT 16 hr/vehicle, $p = 2.06 \times 10^{-27}$).

at the *PSA*, *KLK2* and *TMPRSS2* genes (Figure S4) (Schuur et al., 1996; Sun et al., 1997; Wang et al., 2007; Yu et al., 1999). We next compared AR binding in two cell lines using a less stringent statistical cutoff ($p < 1 \times 10^{-4}$ or FDR 15%) to avoid missing true differential binding sites with low binding affinity (MAT score). LNCaP cells have a greater number of higher affinity AR binding sites than do abl cells (Figures 2A and S5), which is consistent with a previous report showing that androgen signaling activity is significantly decreased in AIPC compared with ADPC (Tomlins et al., 2007). Correlation of AR binding sites with activated and basal AR-regulated genes showed a significant enrichment of AR binding within 20–50 kb of the transcription start sites (TSS) of upregulated genes but not of downregulated genes in both ADPC and AIPC (Figures 2B and S6), suggesting that these upregulated genes are primarily direct targets of AR action.

Although in general the level AR occupancy at target sites is greater in LNCaP cells than in abl cells (Figure 3A), we find greater occupancy of AR binding near abl-specific AR upregulated cell-cycle genes and M-phase genes in abl cells than in LNCaP cells (Figure 3A and Table S2). Greater levels of AR binding are correlated with higher expression of target cell-cycle and M-phase genes in abl (Figure 3B and Table S2). Directed ChIP for the AR binding sites near the M-phase cell-cycle regulatory genes *CDC20*, *UBE2C*, *CDK1*, and *ANAPC10* confirmed that these sites are preferentially occupied in abl as compared with LNCaP in the presence of DHT and have significant AR occupancy in the absence of hormone only in abl and not in LNCaP (Figure 3C). We examined the mRNA (Figure 3D) and protein (Figure 3E) expression of *CDC20*, *UBE2C*, and *CDK1* in abl and LNCaP cells in the absence of hormone and following AR silencing. These results confirmed that these genes are differentially upregulated and AR-dependent in abl as compared with LNCaP.

Selective Active Epigenetic Marks and Collaborating Transcription Factors at M-Phase Gene Enhancers Lead to Increased AR Occupancy at These Sites in AIPC

Among the specific AR regulated M-phase cell-cycle genes in abl cells, ubiquitin-conjugating enzyme E2C (UBE2C), an anaphase-promoting complex (APC)-specific ubiquitin-conjugating enzyme, is of particular interest as the expression of this gene was recently found to be critical for inactivating the cell-cycle M-phase checkpoint (Reddy et al., 2007). Therefore, we further characterized the two specific UBE2C AR binding sites that are located −32.8 kb and +41.6 kb away from the TSS of *UBE2C* gene in abl cells (Figure S7). While these two putative enhancers are within or downstream of other annotated genes, *UBE2C* is the only AR dependent gene in the region. In order to test whether these two putative enhancers communicate with the UBE2C promoter, we performed quantitative chromosome conformation capture assays (3C-qPCR) (Hagege et al., 2007). Fixed chromatin from LNCaP and abl cells treated with DHT or vehicle was digested with BglII followed by ligation under low DNA concentrations and reverse

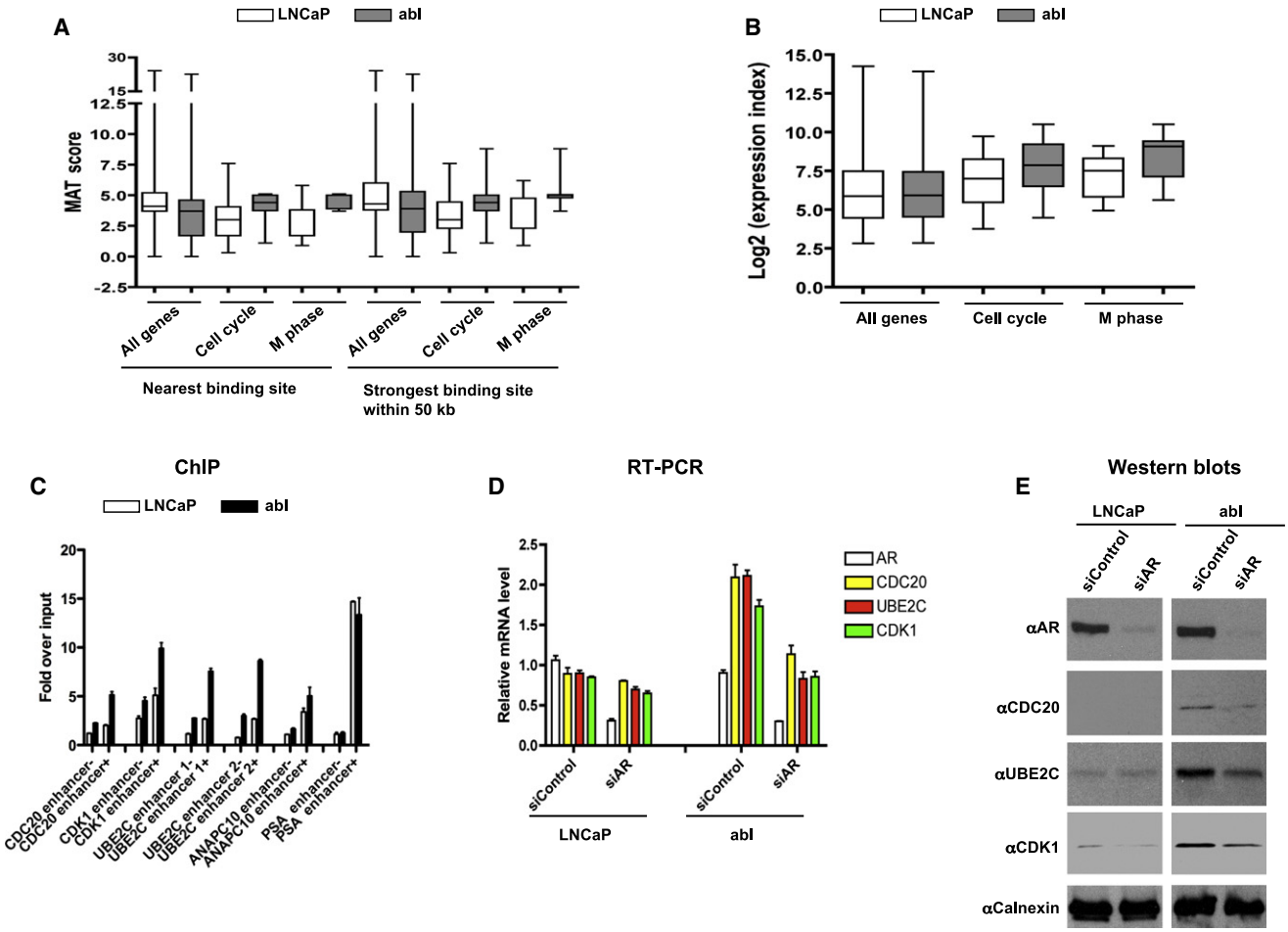

Figure 3. Higher Occupancy of AR Binding Near the M-Phase Cell-Cycle Genes Leads to Higher Expression Levels of These Genes in abl Cells

(A) Comparison of MAT score of the nearest and the strongest AR binding site within 50 kb of all genes, basal AR upregulated cell-cycle genes and M phase genes in LNCaP and abl cells. The difference of all genes and M-phase genes between two cell lines is statistically significant (t test on two independent samples, means ± SE, nearest binding site (all genes, abl/LNCaP = 0.78-fold, $p = 2.17 \times 10^{-154}$, M-phase genes, abl/LNCaP = 1.75-fold, $p = 5.85 \times 10^{-4}$), strongest binding site (all genes, abl/LNCaP = 0.8-fold, $p = 2.48 \times 10^{-127}$, M-phase genes, abl/LNCaP = 1.64-fold, $p = 6.29 \times 10^{-3}$).

(B) Comparison of gene expression index of all genes, basal AR upregulated cell-cycle and M-phase genes in abl cells. Significant difference is observed between cell-cycle and M-phase gene expression in two cell lines (t test on two independent samples, means ± SE, cell cycle, 1.13-fold, $p = 4.51 \times 10^{-3}$, M-phase 1.18-fold, $p = 2.65 \times 10^{-3}$).

(C) ChIP analysis of AR recruitment to various AR binding sites near cell-cycle genes. The PSA enhancer was used as a positive control. ChIP assays were performed with anti-AR antibodies in the presence (+) and absence (-) of DHT. (mean [n = 2) ± SE).

(D) AR silencing specifically decrease high expression of M-phase genes *CDC20*, *UBE2C* and *CDK1* in abl cells. Seventy-two hours after siRNA transfection into LNCaP and abl cells in the absence of DHT, total RNA was isolated and amplified by real-time RT-PCR using gene specific primers (mean [n = 3] ± SE).

(E) AR silencing specifically decreases high protein expression levels of CDC20, UBE2C and CDK1 in abl cells. Western blots were performed using the antibodies indicated ninety-six hours after siRNA transfection into LNCaP and abl cells without DHT.

crosslinking. The ligation products were quantified using Taqman real-time PCR. This revealed significantly greater interaction between these two putative enhancers and the UBE2C promoter in abl cells than in LNCaP cells in the absence of hormone (Figure 4A). In order to determine the mechanism of the preferential occupancy of the UBE2C enhancer sequences in abl we examined whether there were abl-specific sequence alterations in these regions. Sequencing of the two UBE2C enhancer regions identified by AR ChIP-on-chip in LNCaP and abl cells revealed that these two regions are 100% identical in the two cell lines (data not shown).

Given our previous findings that collaborating transcription factors and coactivators may assist nuclear receptor binding in certain regions (Carroll et al., 2005; Shao et al., 2004; Wang et al., 2007), we then investigated whether the previously identified AR collaborating factors FoxA1, GATA2 and Oct1 (Wang et al., 2007) and AR coactivator MED1 (TRAP220) (Wang et al., 2005, 2002) are differentially recruited to the UBE2C enhancers in two cell lines. Directed ChIP analysis showed significantly higher occupancy of FoxA1 and MED1 to both enhancers and GATA2 to enhancer 2 in abl cells as compared with LNCaP cells

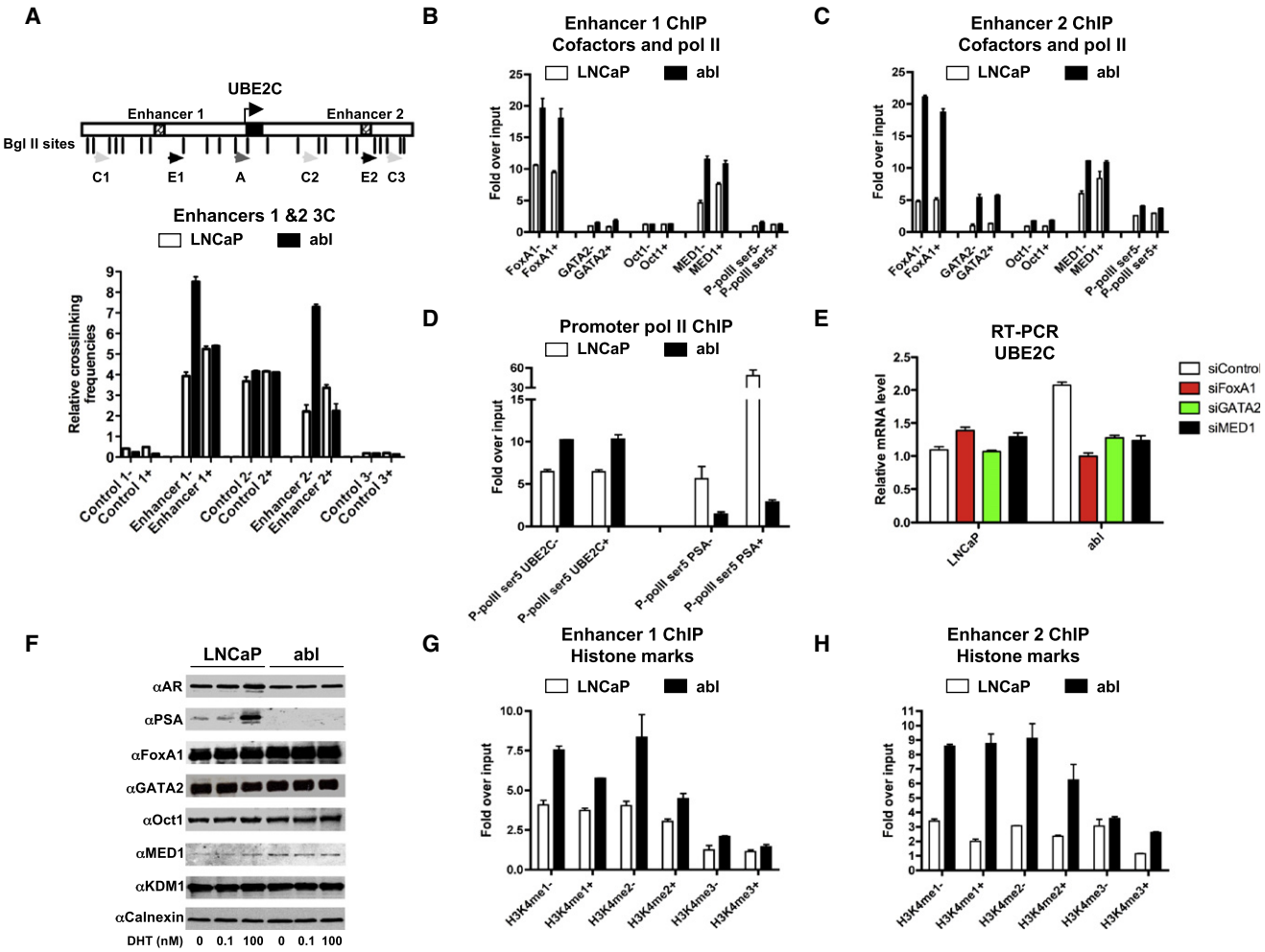

Figure 4. Higher Levels of Active Epigenetic Histone Marks and Recruitment of Collaborating Factors Are Correlated with Greater AR Occupancy on the UBE2C Enhancers in abl Cells

(A) Upper panel: Schematic diagram showing the UBE2C locus. The arrows indicate the location and the direction of primers used in the 3C-qPCR assays. The anchor primer (A) and the Taqman probe were designed in the BglII fragment containing the UBE2C promoter. All other test primers (C1, C2, C3, E1, and E2) were designed within 50 bp to the restriction sites. Lower panel: The two UBE2C enhancers interact with the UBE2C promoter in abl cells. 3C assays were performed using BglII enzyme in LNCaP and abl cells in the presence (+) and absence (−) of DHT (mean [n = 2] ± SE).

(B and C) Stronger FoxA1 and MED1 binding to the UBE2C enhancer 1 and FoxA1, GATA2 and MED1 binding to the UBE2C enhancer 2 in abl cells than in LNCaP cells. ChIP assays were performed using antibodies against FoxA1, GATA2, Oct1, MED1 and P-pol II ser 5 in LNCaP and abl cells treated with (+) and without (−) androgen (mean [n = 2] ± SE).

(D) Higher p-pol II ser 5 occupancy on the UBE2C promoter in abl cells than in LNCaP cells. P-pol II ser 5 binding at the PSA promoter was served as a control. ChIP assays were conducted in LNCaP and abl cells in the presence (+) and absence (−) of DHT using an anti-p-pol II ser 5 antibody (mean [n = 2] ± SE).

(E) Effects of siRNA on UBE2C gene expression in LNCaP and abl cells. Real-time PCR was performed seventy-two hours after siRNA transfection in the absence of DHT (mean [n = 3] ± SE).

(F) Comparison of protein expression in LNCaP and abl cells by western blots. Western blots analyses were performed comparing AR, PSA, FoxA1, GATA2, Oct1, MED1, and KDM1 protein expression levels in the absence and presence of DHT (0.1 nM and 100 nM).

(G and H) UBE2C enhancers 1 (G) and 2 (H) have higher H3K4me1 and H3K4me2 levels in abl cells than in LNCaP cells. Levels of H3K4 me1, H3K4me2 and H3K4me3 on UBE2C enhancers were determined by ChIP assays in the presence (+) and absence (-) of DHT using specific antibodies against H3K4 me1, H3K4me2 and H3K4me3 (mean [n = 2] ± SE).

(Figures 4B and 4C). We also examined serine 5 phosphorylated polymerase II (P-pol II ser 5) occupancy at the UBE2C promoter in both cell lines (Figure 4D). We find significantly greater P-pol II ser 5 occupancy at the UBE2C promoter in abl compared with LNCaP cells that is unchanged by the addition of DHT. In contrast, at the PSA promoter P-pol II ser 5 occupancy is significantly greater in LNCaP cells and is stimulated by DHT. The greater level of AR transcription complex loading on the UBE2C enhancers leads to a greater level of P-pol II ser 5 at the promoter through chromosomal looping (Figure 4A), resulting in higher UBE2C expression levels in abl cells (Figures 3D and 4E). Importantly, silencing of FoxA1, GATA2 or MED1 decreases UBE2C

mRNA level in abl cells but not in LNCaP cells (Figure 4E), suggesting that each of these factors plays an indispensable role in mediating UBE2C expression.

Interestingly, while minimally greater levels MED1 protein expression in abl (Figure 4F) might account for greater MED1 recruitment to the UBE2C enhancers, differences in expression do not account for the differential recruitment of FoxA1 and GATA2 to the UBE2C enhancers. We have recently defined a role for the active enhancer histone marks H3 lysine 4 mono- and di-methyl (H3K4me1 and H3K4me2) (Bernstein et al., 2005; Heintzman et al., 2007) in specifying sites of FoxA1 recruitment in various cell types (Lupien et al., 2008), we therefore examined the levels of these marks (and as control the promoter-specific H3K4me3 mark) at the UBE2C enhancers. We find that H3K4me1 and H3K4me2 are significantly enriched at the UBE2C enhancers only in abl and not in LNCaP (Figures 4G and 4H) suggesting that these epigenetic marks may define these sites as abl-specific enhancers leading to AR-dependent expression of UBE2C only in this cell type.

In order to determine whether H3K4 methylation is required for the increased AR occupancy at the UBE2C enhancers in abl cells we overexpressed a H3K4me1 and H3K4me2 specific demethylase KDM1 (Shi et al., 2004) in both LNCaP and abl cells. Consistent with our recent finding that KDM1 overexpression reduces FoxA1 recruitment in MCF7 cells (Lupien et al., 2008), we found that KDM1 overexpression decreases FoxA1 binding and H3K4me2 level at the UBE2C enhancers (Figure S8). More significantly, overexpression of KDM1 almost completely abolishes AR binding in both cell lines (Figure 5A), suggesting that H3K4 marks are required for differential AR binding at the UBE2C enhancers in LNCaP and abl cells. Interestingly, FoxA1 silencing also almost fully abolishes AR binding at the UBE2C enhancers in LNCaP and abl cells (Figure 5B), suggesting FoxA1 binding is also essential for differential AR recruitment. By contrast, silencing of AR has no effect on differential H3K4me2 level and FoxA1 binding on the UBE2C enhancers (Figure 5C). In addition, FoxA1 silencing has no effect on differential H3K4me2 levels on the UBE2C enhancers (Figure S9). Thus the differential H3K4 marks and FoxA1 act upstream of AR and are required for differential AR binding at the UBE2C enhancers (Figure 5D).

To confirm that the requirement for H3K4 methylation and FoxA1 binding for AR binding was not restricted to the UBE2C enhancers, we performed H3K4me1, H3K4me2 and FoxA1 ChIP on the CDK1, CDC20 and ANAPC10 enhancers. We find that the levels of H3K4 methyl marks and FoxA1 are also higher on these enhancers in abl cells than LNCaP cells (Figure S10). As controls, the H3K4 marks and FoxA1 are not present at randomly selected androgen responsive elements (ARE) that have no AR binding (Figure S10). As expected, overexpression of KDM1 or silencing of FoxA1 also significantly decreases AR binding on the CDK1 and CDC20 enhancers (Figure S11). Moreover, overexpression of UBE2C does not increase AR binding at the CDK1, CDC20 and ANAPC10 enhancers in LNCaP cells (Figure S12). These findings suggest that increased AR binding at the enhancers of other M-phase genes in abl cells is also determined by H3K4 methylation and FoxA1 binding rather than being the result of increased UBE2C expression.

Higher Levels of H3K4 Methylation and FoxA1 Binding at the UBE2C Enhancers Leads to Overexpression of UBE2C Protein in AIPC Cases

In order to confirm that AR-dependent overexpression of UBE2C is not unique to abl cells, we determined UBE2C protein expression levels in another model of AIPC and in clinical AIPC cases. We confirmed that UBE2C protein level is greater and AR-dependent in the androgen-independent cell line C4-2B (Thalmann et al., 2000) than in LNCaP (Figure S13). More significantly we examined UBE2C protein expression in clinical cases of AIPC. We measured by immunohistochemistry UBE2C protein levels in tissue microarrays containing normal prostate, ADPC and AIPC tissues (n = 372 tissue microarray elements). AIPC samples showed strong UBE2C staining, whereas weak and no staining was observed in ADPC and normal prostate, respectively (Figures 6A and 6B). These data suggest that UBE2C protein overexpression correlates with the occurrence and progression of prostate cancer.

To investigate whether the overexpression of UBE2C protein in clinical samples is also caused by enhanced AR transcription complex occupancy at the UBE2C enhancers, we performed AR, FoxA1, H3K4me1 and H3K4me2 ChIP using tissues from ADPC and AIPC cases. We found significantly greater AR and FoxA1 occupancy and H3K4 methylation at the UBE2C enhancers in a case of AIPC as compared with an ADPC case (Figure S14). While limited by the number of available cases for analysis, this finding is consistent with our findings in LNCaP and abl and supports the conclusion that increased H3K4 methylation and FoxA1 and AR occupancy at the UBE2C enhancers leads to increased UBE2C expression in AIPC.

Functional Role of UBE2C in AIPC Growth

Finally, we explored the functional role of UBE2C in prostate cancer growth. Although overexpression of UBE2C in LNCaP cells is not sufficient to accelerate LNCaP cell grow in the absence of androgen (Figure S15), silencing of UBE2C selectively decreases abl (two-side t test, $p = 9.1 \times 10^{-3}$) but not LNCaP cell proliferation (Figure 7A), suggesting that UBE2C is necessary for abl cell proliferation in the absence of hormone (Figures 7A and S1A). The UBE2C protein half-life of ~6 hr in both LNCaP and abl cells (Figure S16) suggests that it is AR-dependent androgen-independent upregulation *UBE2C* transcription (Figures 4–6 and S14) rather than a more stable UBE2C protein that contributes to its increased level and the increased growth of abl cells in the absence of androgen.

Consistent with the critical role of UBE2C in inactivating the M-phase checkpoint (Reddy et al., 2007), fluorescence-activated cell sorting (FACS) analysis revealed that silencing of UBE2C causes a G2/M accumulation in both cell lines (Figure 7B). As previously reported, AR silencing leads to a G1/S block in LNCaP cells (Comstock and Knudsen, 2007), however it leads to a G2/M block in abl cells (Figure 7B). This increase in G2/M phase cells was further confirmed by an increase in histone H3 serine 10 phosphorylation (P-H3Ser10) level (Figure 7C) that peaks in metaphase (Prigent and Dimitrov, 2003). Interestingly, silencing of UBE2C in both LNCaP and abl cells also led to an increase S phase (Figure 7B), which could caused by either a S phase block or a shortened G1. To distinguish between these two

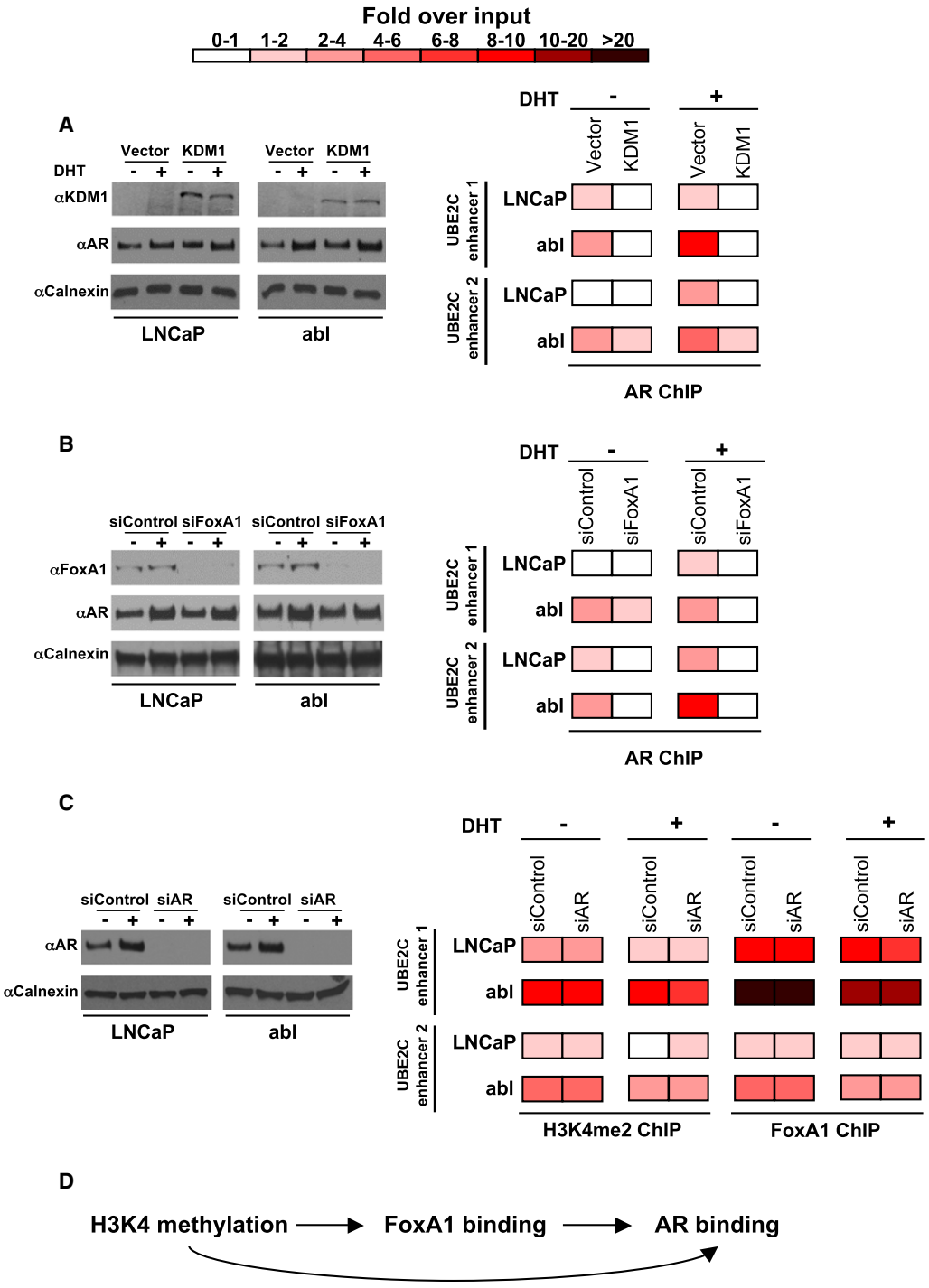

Figure 5. H3K4me2 and FoxA1 Act Upstream of AR and Are Required for Differential AR Binding in abl Cells

(A) Overexpression of KDM1 abolishes differential AR binding in LNCaP and abl cells. Cells were transfected with a FLAG-tagged KDM1 vector or an empty vector control. Three days after transfection, cells were treated with (+) or without (-) DHT. AR ChIP was then performed on the UBE2C enhancers. The overexpression of KDM1 levels was monitored by western blot.

(B) FoxA1 silencing abolishes differential AR binding in LNCaP and abl cells. Cells were transfected with siFoxA1. AR ChIP was then performed in the presence (+) and absence (–) of DHT on the UBE2C enhancers. The reduction of FoxA1 protein level was verified by western blot.

(C) AR silencing has no effect on differential H3K4me2 level and FoxA1 recruitment. Cells were transfected with siAR. H3K4me2 and FoxA1 ChIP were then performed in the presence (+) and absence (-) of DHT on the UBE2C enhancers. The reduction of AR protein was demonstrated by western blot.

(D) A hierarchical model for AR action on the UBE2C enhancers. H3K4 methylation and FoxA1 act upstream of AR, and H3K4 methylation functions upstream of FoxA1.

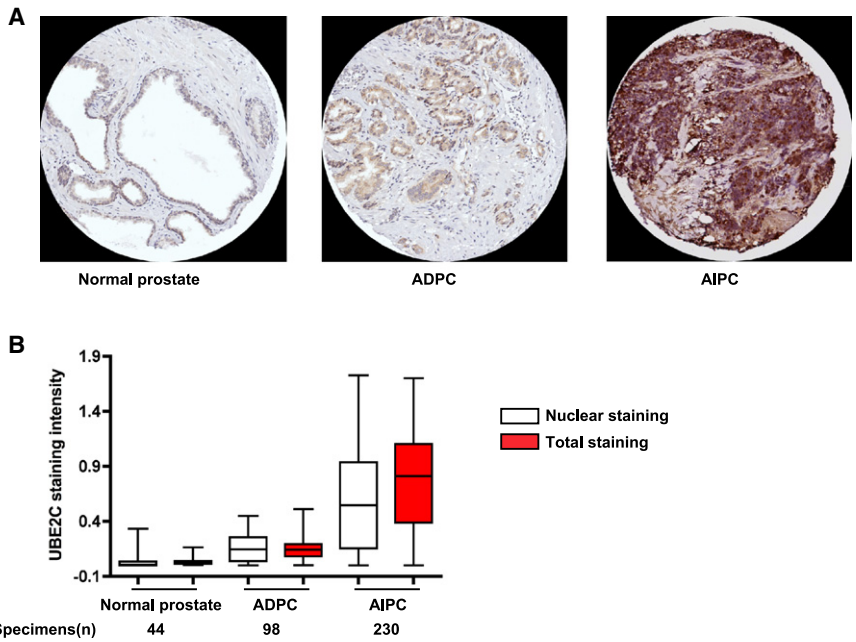

Figure 6. UBE2C Protein Expression Level Is Overexpressed in AIPC Cases

(A) Representative tissue microarray elements stained with an antibody against UBE2C (magnification 20×). Stronger staining of UBE2C was seen in AIPC than in ADPC.

(B) Analysis of UBE2C protein expression in normal prostate, ADPC and AIPC. Tissue microarrays were scanned and scored using the Ariol image analysis system. Nuclear staining and total staining reflect a combination of the percentage of positive nuclei and the intensity of the stain, and a combination of the positive area score and the intensity of the stain, respectively. AIPC has stronger nuclear staining and total staining than ADPC (Welch one-side t test, $p < 2.2 \times 10^{-16}$ for both staining scores). ADPC has higher nuclear staining and total staining scores compared with normal prostate ($p = 5.80 \times 10^{-13}$, $p < 2.2 \times 10^{-16}$, respectively).

possibilities, we synchronized siControl and siUBE2C transfected LNCaP and abl cells in G0 by serum starvation. Cells were then released into cell cycle by the addition of serum. We measured cyclin A protein level over time as this cyclin is not detected during early G1, accumulates at the end of G1 and is essential for G1/S transition (Girard et al., 1991; Resnitzky et al., 1995). Interestingly, we found that Cyclin A accumulated 2 hr earlier in siUBE2C transfected (12 hr) than in siControl transfected (14 hr) LNCaP cells (Figure 7D). In contrast, Cyclin A was detected at the same time point (14 hr) in siUBE2C and siControl transfected abl cells (Figure 7D). These data suggest that UBE2C silencing results in a shortened G1 phase in LNCaP but not in abl cells. Thus the increased S phase fraction observed upon UBE2C silencing (Figure 6B) is likely a result of a delayed S phase in abl cells and shortened G1 phase in LNCaP cells. This may explain why silencing of UBE2C decreases abl but not LNCaP proliferation, even though UBE2C silencing results in G2/M block in both cell lines. The more significant effect CDK1 and CDC20 silencing on cell proliferation in abl cells than in LNCaP cells (Figure S17) may also be the result of a similar mechanism.

DISCUSSION

AR has been found to play a critical role in the development of both ADPC and most cases of AIPC (Debes and Tindall, 2004; Feldman and Feldman, 2001; Heinlein and Chang, 2004). In ADPC, AR promotes cell proliferation through regulation of the cell cycle G1/S transition only in the presence of androgen (Comstock and Knudsen, 2007). In contrast, in AIPC, AR is thought to remain active through a variety of potential mechanisms including AR amplification, AR mutation, increased androgen sensitivity, local androgen production and growth factor activation (Debes and Tindall, 2004; Feldman and Feldman, 2001; Heinlein and Chang, 2004). However, which of these mechanisms is operant and how the "activated" AR regulates AIPC growth is poorly understood. In this study, using cell line models of AIPC and gene expression data and tissue from actual AIPC cases, we find that the program of gene expression regulated by AR in the absence of hormone is distinct from the androgen-regulated program in ADPC.

In contrast to a differentiated prostate program regulated by androgens in LNCaP, AR regulates mitotic cell-cycle genes in abl raising the question as to how this different AR-dependent program is executed in abl cells. Through an integrated analysis of AR cistrome and gene expression data, we found that upregulated genes including cell-cycle genes in abl cells are direct AR direct targets (Figure 2B). By analyzing the epigenetic marks and collaborating transcription factors present at the AR bound M-phase gene enhancers we explored the mechanisms underlying the reprogrammed AR action in both a AIPC model system and clinical cases of AIPC. We found levels of active H3K4 methyl marks and recruitment of other transcription factors including FoxA1 at AR target enhancers, most notably the UBE2C enhancers. Although increased H3K4 methylation may lead to increased recruitment of FoxA1 to facilitate greater AR occupancy (Figures S8 and 5), these active histone marks may also act upstream of other transcription factors and coactivators (e.g., GATA2 and MED1) or directly on AR resulting in increased AR binding at these sites in AIPC. It is also possible that other active histone marks present on gene enhancers (Barski et al., 2007) may play a role to facilitate transcription factor and coactivator recruitment. Interestingly, while silencing of FoxA1 does not affect AR target genes *PSA* and *TMPRSS2* expression and androgen-induced cell-cycle progression in LNCaP cells (Wang et al., 2007), FoxA1 function is required for *UBE2C* expression in abl cells, suggesting that FoxA1 may play a more important role in AIPC than in ADPC.

The finding that differential H3K4 marks are required for differential AR binding raises the question of what are the mechanisms responsible for the establishment of the differential histone marks

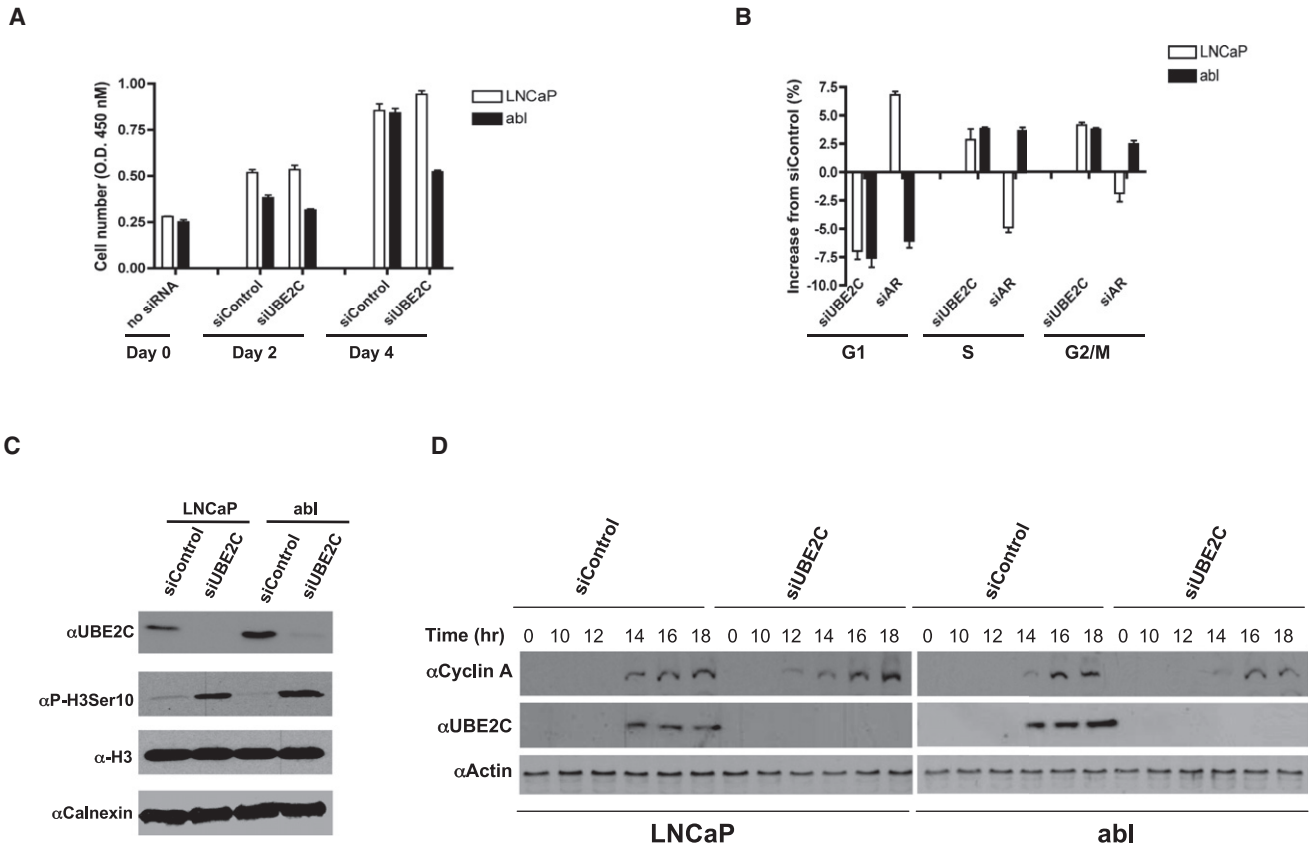

Figure 7. UBE2C Silencing Selectively Decreases abl Cell Growth

(A) Silencing of UBE2C selectively decreases abl cell proliferation. LNCaP and abl were plated as described in Figure 1.The cell proliferation was measured on day 2 and day 4 after siRNA transfection using the WST-1 assay (mean [n = 3] ± SE).

(B) Silencing of UBE2C increases G2/M and S phase cells in LNCaP and abl cells. Ninety-six hr after siRNAs transfection in the absence of DHT, cells were analyzed by FACS (mean [n = 2] ± SE).

(C) Silencing of UBE2C leads to a prolonged mitosis as indicated by P-H3Ser10. Ninety-six hr post siRNAs transfection in the absence of DHT, western blots were performed with histone extraction (for P-H3Ser10 and total H3) or whole-cell lysate (for UBE2C and calnexin) using the antibodies indicated.

(D) UBE2C silencing results in a shortened G1 in LNCaP cells but not in abl cells. LNCaP and abl cells were transfected with siControl or siUBE2C in the absence of DHT. After 6–8 hr, cells were synchronized in G0 by serum starvation for 24 hr. Cells were stimulated to re-enter cell cycle by the addition of 20% serum and harvested at the indicated time points. Cell lysates were subjected to western blot with the indicated antibodies.

in AIPC versus ADPC. It is possible that the expression of H3K4 histone methyltransferases is higher in AIPC than in ADPC. Alternatively, it is conceivable that the specific mechanisms for recruiting the enzymes that make these marks exist in AIPC but not in ADPC (Kouzarides, 2007; Ruthenburg et al., 2007). Future studies will be needed to address these possibilities.

Our findings that AR selectively and directly upregulates M-phase genes in AIPC may explain why maximal androgen blockade that combines AR antagonists with LHRH inhibitors cannot prolong AIPC patient survival (Group, 2000) as such therapies will only inhibit the ability of androgen-bound AR to promote G1/S transition in ADPC but cannot prevent un-liganded AR from accelerating M-phase transition in AIPC. Interestingly, two recent clinical trials have shown that docetaxel, which disrupts mitosis by inhibiting the depolymerization of microtubules, can modestly improve survival of AIPC patients (Petrylak et al., 2004; Tannock et al., 2004), supporting an important role of M-phase in AIPC progression.

Among the M-phase regulatory genes controlled by AR in AIPC we find that UBE2C protein is overexpressed in AIPC cases. Interestingly, UBE2C has also been found to be overexpressed in breast, lung, ovary, bladder, thyroid and esophageal carcinomas (Lin et al., 2006; Pallante et al., 2005; Wagner et al., 2004), suggesting a general role of UBE2C in accelerating M-phase transition in solid tumors. Importantly, silencing of UBE2C significantly decreases AIPC growth by arresting G2/M and S phases, providing a potential new target for therapeutic intervention.

EXPERIMENTAL PROCEDURES

Cell Lines and Samples

The prostate cancer cell line LNCaP was obtained from the American Type Culture Collection. abl cell line was provided by Zoran Culig (Innsbruck Medical University, Austria) (Culig et al., 1999). C4-2B cell line was obtained from ViroMed Laboratories (Minneapolis, MN). The prostate cancer tissue microarrays that include 44 normal prostate specimens, 98 ADPC specimens, and 230 AIPC specimens were obtained from Arul Chinnaiyan (University of

Michigan, MI) and Mark Rubin (Cornell University, NY) as previously described (Rubin et al., 2002). One ADPC tissue and one AIPC tissue used for tissue ChIP were obtained form Arul Chinnaiyan.

Cell Proliferation Assay

Cell proliferation was determined using a WST-1 kit (Roche, Indianapolis, IN).

RNA Interference

A control siRNA (siControl) and siRNA targeting AR, CDC20, UBE2C, and CDK1 (ON TARGET plus™ siRNA) were purchased from Dharmacon (Dharmacon, Lafayette, CO). A second siAR has been described (Haag et al., 2005). siRNA transfections were performed using Lipofectamine 2000 (Invitrogen, Carlsbad, CA). The siRNA sequences were listed in Table S1.

Gene Expression Experiments and Analyses

Hormone-depleted LNCaP and abl cells were transfected with siControl or siAR and abl cells were treated with 100 nM DHT or vehicle. Seventy-two hours after siRNA transfection or four and sixteen hours after DHT treatment, total RNA was isolated using an RNeasy kit (QIAGEN, Valencia, CA). Biological triplicate total RNA was hybridized to Affymetrix human U133 plus 2.0 expression array (Affymetrix, Santa Clara, CA) at the Dana-Farber Cancer Institute (DFCI) Microarray Core Facility. Microarray data have been submitted to the Gene Expression Omnibus (GEO) repository under the accession number GSE11428. The expression raw data for LNCaP cells in the presence or absence of androgen was from our previous work (Wang et al., 2007) (GEO dataset GSE7868). Two clinical ADPC/AIPC expression data were retrieved from GSE3325 and obtained from Steve Balk. All gene expression data was normalized and summarized with RMA algorithm (Irizarry et al., 2003) and an updated RefSeq probe definition (Dai et al., 2005). Significance Analysis of Microarrays (SAM) algorithm (Tusher et al., 2001) was used to detect the differentially expressed genes and calculate the q-values (False Discovery Rate). Genes with q-value less than 0.05 was used to select the differentially expressed genes. Two-way hierarchical clustering analysis was performed to group both gene expression changes (rows) and conditions (columns). Gene Ontology (GO) analysis was performed using the web tool Database for Annotation, Visualization and Integrated Discovery (DAVID) (http://david.abcc.ncifcrf.gov/).

ChIP-on-Chip and Standard ChIP Assays

AR ChIP was performed as previously described (Wang et al., 2007). The ChIP-enriched DNA was amplified, labeled, and hybridized to Affymetrix Human Tiling 2.0R Array Set. Biological triplicate experiments were performed. The ChIP-on-chip raw data are accessible at http://research.dfci.harvard.edu/brownlab/datasets/. ChIP-on-chip data were analyzed using MAT algorithm (Johnson et al., 2006). Antibodies used for ChIP are available in the Supplemental Experimental Procedures.

Correlation of AR Binding to Gene Expression

Genes having AR binding sites within certain distance were defined as those having at least one such site within the distance relative to the transcription start sites. For each category of AR-regulated genes, the percentage of genes having AR binding sites in LNCaP or abl cells within 20–100 kb was calculated. All RefSeq genes in Affymetrix human U133 plus 2.0 expression array were used as the control category. Chi-square test was used to assess the statistical significance for the percentages of AR-regulated genes having AR binding sites.

Real-Time RT-PCR

Real-time RT-PCR was performed as before (Wang et al., 2007). Primers used are listed in Table S1.

Western Blots

Western blots were performed as previously described (Wang et al., 2002). Antibodies used are available in the Supplemental Experimental Procedures.

Quantitative Chromosome Conformation Capture Assay

3C-qPCR assays were performed essentially as described (Hagege et al., 2007) with minor modifications. Details are available in the Supplemental Experimental Procedures.

Tissue Microarray Analysis

The immunohistochemistry of UBE2C on tissue microarrays was performed as described (Wang et al., 2008) using anti-UBE2C (A650) at 1:600 dilution. Details are available in the Supplemental Experimental Procedures.

Fluorescence-Activated Cell Sorting Analysis

siRNA transfected LNCaP and abl cells were collected, stained with propidium iodide and DNA contents were analyzed by DFCI Cytometry Core Facility.

SUPPLEMENTAL DATA

Supplemental Data include Supplemental Experimental Procedures, Supplemental References, seventeen figures, and two tables and can be found with this article online at http://www.cell.com/supplemental/S0092-8674(09)00517-0.

ACKNOWLEDGMENTS

This work was supported by grants from National Institutes of Health (P50 CA090381 to M.B., K99 CA126160 to Q.W., and R01 HG004069 to X.S.L., and K99 CA129565 to J.Y., The Prostate Cancer Foundation (to M.B), and Department of Defense (W81XWH-07-1-0037 to X.S.L., and PC080665 to J.Y.). We thank Drs. Roland Schüle for providing KDM1 constructs; and Michael Rape for UBE2C constructs. We also thank Drs. James DeCaprio, Gustavo Leone, Tim Huang, Yun Li, and Shengjun Ren for helpful discussions; and Dr. Chunpeng Zhang and Anna Rorick for technical assistance.

Received: July 28, 2008
Revised: December 4, 2008
Accepted: April 22, 2009
Published: July 23, 2009

REFERENCES

Barski, A., Cuddapah, S., Cui, K., Roh, T.Y., Schones, D.E., Wang, Z., Wei, G., Chepelev, I., and Zhao, K. (2007). High-resolution profiling of histone methylations in the human genome. Cell *129*, 823–837.

Bernstein, B.E., Kamal, M., Lindblad-Toh, K., Bekiranov, S., Bailey, D.K., Huebert, D.J., McMahon, S., Karlsson, E.K., Kulbokas, E.J., 3rd, Gingeras, T.R., et al. (2005). Genomic maps and comparative analysis of histone modifications in human and mouse. Cell *120*, 169–181.

Carroll, J.S., Liu, X.S., Brodsky, A.S., Li, W., Meyer, C.A., Szary, A.J., Eeckhoute, J., Shao, W., Hestermann, E.V., Geistlinger, T.R., et al. (2005). Chromosome-wide mapping of estrogen receptor binding reveals long-range regulation requiring the forkhead protein FoxA1. Cell *122*, 33–43.

Chen, C.D., Welsbie, D.S., Tran, C., Baek, S.H., Chen, R., Vessella, R., Rosenfeld, M.G., and Sawyers, C.L. (2004). Molecular determinants of resistance to antiandrogen therapy. Nat. Med. *10*, 33–39.

Comstock, C.E., and Knudsen, K.E. (2007). The complex role of AR signaling after cytotoxic insult: implications for cell-cycle-based chemotherapeutics. Cell Cycle *6*, 1307–1313.

Culig, Z., Hoffmann, J., Erdel, M., Eder, I.E., Hobisch, A., Hittmair, A., Bartsch, G., Utermann, G., Schneider, M.R., Parczyk, K., et al. (1999). Switch from antagonist to agonist of the androgen receptor bicalutamide is associated with prostate tumour progression in a new model system. Br. J. Cancer *81*, 242–251.

Dai, M., Wang, P., Boyd, A.D., Kostov, G., Athey, B., Jones, E.G., Bunney, W.E., Myers, R.M., Speed, T.P., Akil, H., et al. (2005). Evolving gene/transcript definitions significantly alter the interpretation of GeneChip data. Nucleic Acids Res. *33*, e175.

Debes, J.D., and Tindall, D.J. (2004). Mechanisms of androgen-refractory prostate cancer. N. Engl. J. Med. *351*, 1488–1490.

Feldman, B.J., and Feldman, D. (2001). The development of androgen-independent prostate cancer. Nat. Rev. Cancer *1*, 34–45.

Girard, F., Strausfeld, U., Fernandez, A., and Lamb, N.J. (1991). Cyclin A is required for the onset of DNA replication in mammalian fibroblasts. Cell *67*, 1169–1179.

Group, P.C.T.C. (2000). Maximum androgen blockade in advanced prostate cancer: an overview of the randomised trials. Lancet *355*, 1491–1498.

Haag, P., Bektic, J., Bartsch, G., Klocker, H., and Eder, I.E. (2005). Androgen receptor down regulation by small interference RNA induces cell growth inhibition in androgen sensitive as well as in androgen independent prostate cancer cells. J. Steroid Biochem. Mol. Biol. *96*, 251–258.

Hagege, H., Klous, P., Braem, C., Splinter, E., Dekker, J., Cathala, G., de Laat, W., and Forne, T. (2007). Quantitative analysis of chromosome conformation capture assays (3C-qPCR). Nat. Protocols *2*, 1722–1733.

Heinlein, C.A., and Chang, C. (2004). Androgen receptor in prostate cancer. Endocr. Rev. *25*, 276–308.

Heintzman, N.D., Stuart, R.K., Hon, G., Fu, Y., Ching, C.W., Hawkins, R.D., Barrera, L.O., Van Calcar, S., Qu, C., Ching, K.A., et al. (2007). Distinct and predictive chromatin signatures of transcriptional promoters and enhancers in the human genome. Nat. Genet. *39*, 311–318.

Irizarry, R.A., Hobbs, B., Collin, F., Beazer-Barclay, Y.D., Antonellis, K.J., Scherf, U., and Speed, T.P. (2003). Exploration, normalization, and summaries of high density oligonucleotide array probe level data. Biostatistics *4*, 249–264.

Johnson, D.S., Li, W., Gordon, D.B., Bhattacharjee, A., Curry, B., Ghosh, J., Brizuela, L., Carroll, J.S., Brown, M., Flicek, P., et al. (2008). Systematic evaluation of variability in ChIP-chip experiments using predefined DNA targets. Genome Res. *18*, 393–403.

Johnson, W.E., Li, W., Meyer, C.A., Gottardo, R., Carroll, J.S., Brown, M., and Liu, X.S. (2006). Model-based analysis of tiling-arrays for ChIP-chip. Proc. Natl. Acad. Sci. USA *103*, 12457–12462.

Kouzarides, T. (2007). Chromatin modifications and their function. Cell *128*, 693–705.

Lin, J., Raoof, D.A., Wang, Z., Lin, M.Y., Thomas, D.G., Greenson, J.K., Giordano, T.J., Orringer, M.B., Chang, A.C., Beer, D.G., et al. (2006). Expression and effect of inhibition of the ubiquitin-conjugating enzyme E2C on esophageal adenocarcinoma. Neoplasia *8*, 1062–1071.

Lupien, M., Eeckhoute, J., Meyer, C.A., Wang, Q., Zhang, Y., Li, W., Carroll, J.S., Liu, X.S., and Brown, M. (2008). FoxA1 translates epigenetic signatures into enhancer-driven lineage-specific transcription. Cell *132*, 958–970.

Mangelsdorf, D.J., Thummel, C., Beato, M., Herrlich, P., Schutz, G., Umesono, K., Blumberg, B., Kastner, P., Mark, M., Chambon, P., et al. (1995). The nuclear receptor superfamily: the second decade. Cell *83*, 835–839.

Pallante, P., Berlingieri, M.T., Troncone, G., Kruhoffer, M., Orntoft, T.F., Viglietto, G., Caleo, A., Migliaccio, I., Decaussin-Petrucci, M., Santoro, M., et al. (2005). UbcH10 overexpression may represent a marker of anaplastic thyroid carcinomas. Br. J. Cancer *93*, 464–471.

Petrylak, D.P., Tangen, C.M., Hussain, M.H., Lara, P.N., Jr., Jones, J.A., Taplin, M.E., Burch, P.A., Berry, D., Moinpour, C., Kohli, M., et al. (2004). Docetaxel and estramustine compared with mitoxantrone and prednisone for advanced refractory prostate cancer. N. Engl. J. Med. *351*, 1513–1520.

Prigent, C., and Dimitrov, S. (2003). Phosphorylation of serine 10 in histone H3, what for? J. Cell Sci. *116*, 3677–3685.

Reddy, S.K., Rape, M., Margansky, W.A., and Kirschner, M.W. (2007). Ubiquitination by the anaphase-promoting complex drives spindle checkpoint inactivation. Nature *446*, 921–925.

Resnitzky, D., Hengst, L., and Reed, S.I. (1995). Cyclin A-associated kinase activity is rate limiting for entrance into S phase and is negatively regulated in G1 by p27Kip1. Mol. Cell. Biol. *15*, 4347–4352.

Rubin, M.A., Zhou, M., Dhanasekaran, S.M., Varambally, S., Barrette, T.R., Sanda, M.G., Pienta, K.J., Ghosh, D., and Chinnaiyan, A.M. (2002). alpha-Methylacyl coenzyme A racemase as a tissue biomarker for prostate cancer. JAMA *287*, 1662–1670.

Ruthenburg, A.J., Allis, C.D., and Wysocka, J. (2007). Methylation of lysine 4 on histone H3: intricacy of writing and reading a single epigenetic mark. Mol. Cell *25*, 15–30.

Scher, H.I., and Sawyers, C.L. (2005). Biology of progressive, castration-resistant prostate cancer: directed therapies targeting the androgen-receptor signaling axis. J. Clin. Oncol. *23*, 8253–8261.

Schuur, E.R., Henderson, G.A., Kmetec, L.A., Miller, J.D., Lamparski, H.G., and Henderson, D.R. (1996). Prostate-specific antigen expression is regulated by an upstream enhancer. J. Biol. Chem. *271*, 7043–7051.

Shang, Y., Myers, M., and Brown, M. (2002). Formation of the androgen receptor transcription complex. Mol. Cell *9*, 601–610.

Shao, W., Keeton, E.K., McDonnell, D.P., and Brown, M. (2004). Coactivator AIB1 links estrogen receptor transcriptional activity and stability. Proc. Natl. Acad. Sci. USA *101*, 11599–11604.

Shi, Y., Lan, F., Matson, C., Mulligan, P., Whetstine, J.R., Cole, P.A., and Casero, R.A. (2004). Histone demethylation mediated by the nuclear amine oxidase homolog LSD1. Cell *119*, 941–953.

Stanbrough, M., Bubley, G.J., Ross, K., Golub, T.R., Rubin, M.A., Penning, T.M., Febbo, P.G., and Balk, S.P. (2006). Increased expression of genes converting adrenal androgens to testosterone in androgen-independent prostate cancer. Cancer Res. *66*, 2815–2825.

Sun, Z., Pan, J., and Balk, S.P. (1997). Androgen receptor-associated protein complex binds upstream of the androgen-responsive elements in the promoters of human prostate-specific antigen and kallikrein 2 genes. Nucleic Acids Res. *25*, 3318–3325.

Tannock, I.F., de Wit, R., Berry, W.R., Horti, J., Pluzanska, A., Chi, K.N., Oudard, S., Theodore, C., James, N.D., Turesson, I., et al. (2004). Docetaxel plus prednisone or mitoxantrone plus prednisone for advanced prostate cancer. N. Engl. J. Med. *351*, 1502–1512.

Thalmann, G.N., Sikes, R.A., Wu, T.T., Degeorges, A., Chang, S.M., Ozen, M., Pathak, S., Chung, L.W., et al. (2000). LNCaP progression model of human prostate cancer: androgen-independence and osseous metastasis. Prostate *44*, 91–103.

Tomlins, S.A., Mehra, R., Rhodes, D.R., Cao, X., Wang, L., Dhanasekaran, S.M., Kalyana-Sundaram, S., Wei, J.T., Rubin, M.A., Pienta, K.J., et al. (2007). Integrative molecular concept modeling of prostate cancer progression. Nat. Genet. *39*, 41–51.

Tusher, V.G., Tibshirani, R., and Chu, G. (2001). Significance analysis of microarrays applied to the ionizing radiation response. Proc. Natl. Acad. Sci. USA *98*, 5116–5121.

Varambally, S., Yu, J., Laxman, B., Rhodes, D.R., Mehra, R., Tomlins, S.A., Shah, R.B., Chandran, U., Monzon, F.A., Becich, M.J., et al. (2005). Integrative genomic and proteomic analysis of prostate cancer reveals signatures of metastatic progression. Cancer Cell *8*, 393–406.

Wagner, K.W., Sapinoso, L.M., El-Rifai, W., Frierson, H.F., Butz, N., Mestan, J., Hofmann, F., Deveraux, Q.L., and Hampton, G.M. (2004). Overexpression, genomic amplification and therapeutic potential of inhibiting the UbcH10 ubiquitin conjugase in human carcinomas of diverse anatomic origin. Oncogene *23*, 6621–6629.

Wang, H., Leav, I., Ibaragi, S., Wegner, M., Hu, G.F., Lu, M.L., Balk, S.P., and Yuan, X. (2008). SOX9 is expressed in human fetal prostate epithelium and enhances prostate cancer invasion. Cancer Res. *68*, 1625–1630.

Wang, Q., Carroll, J.S., and Brown, M. (2005). Spatial and temporal recruitment of androgen receptor and its coactivators involves chromosomal looping and polymerase tracking. Mol. Cell *19*, 631–642.

Wang, Q., Li, W., Liu, X.S., Carroll, J.S., Janne, O.A., Keeton, E.K., Chinnaiyan, A.M., Pienta, K.J., and Brown, M. (2007). A hierarchical network of transcription factors governs androgen receptor-dependent prostate cancer growth. Mol. Cell *27*, 380–392.

Wang, Q., Sharma, D., Ren, Y., and Fondell, J.D. (2002). A coregulatory role for the TRAP-mediator complex in androgen receptor-mediated gene expression. J. Biol. Chem. *277*, 42852–42858.

Xu, Y., Chen, S.Y., Ross, K.N., and Balk, S.P. (2006). Androgens induce prostate cancer cell proliferation through mammalian target of rapamycin activation and post-transcriptional increases in cyclin D proteins. Cancer Res. *66*, 7783–7792.

Yu, D.C., Sakamoto, G.T., and Henderson, D.R. (1999). Identification of the transcriptional regulatory sequences of human kallikrein 2 and their use in the construction of calydon virus 764, an attenuated replication competent adenovirus for prostate cancer therapy. Cancer Res. *59*, 1498–1504.